

Communication

Mechanical Alloying Synthesis of Co₉S₈ Particles as Materials for Supercapacitors

Bo Li ¹, Yuxia Hu ², Jiajia Li ³, Maocheng Liu ^{1,3,*}, Lingbin Kong ¹, Yumei Hu ¹ and Long Kang ¹

¹ School of Materials Science and Engineering, Lanzhou University of Technology, Lanzhou 730050, China; ascend1994@163.com (B.L.); konglb@lut.cn (L.K.); huyumeiu@163.com (Y.H.); kangl@lut.cn (L.K.)

² School of Bailie Engineering & Technology, Lanzhou City University, Lanzhou 730070, China; huyuxiav@163.com

³ State Key Laboratory of Advanced Processing and Recycling of Non-ferrous Metals, Lanzhou University of Technology, Lanzhou 730050, China; 15117180719@163.com

* Correspondence: liumc@lut.cn; Tel.: +86-931-2976579

Academic Editor: Chun-Liang Chen

Received: 6 May 2016; Accepted: 31 May 2016; Published: 16 June 2016

Abstract: Cobalt sulfide (Co₉S₈) particles are compounded as the electrode materials of supercapacitors by a mechanical alloying method. They show excellent properties including good cycling stability and high specific capacitance. A supercapacitor is assembled using Co₉S₈ as the anode and activated carbon (AC) as the cathode. It gains a maximum specific capacitance of 55 F·g⁻¹ at a current density of 0.5 A·g⁻¹, and also an energy density of 15 Wh·kg⁻¹. Those results show that the novel and facile synthetic route may be able to offer a new way to synthesize alloy compounds with excellent supercapacitive properties.

Keywords: Co₉S₈ particle; mechanical alloying; energy storage and conversion; nanoparticles

1. Introduction

As industry and society develop rapidly, it is difficult for natural energy resources to satisfy the requirements. Therefore, we need to jump into action immediately to change this situation. What comforts us is that the invention of a supercapacitor possessing an outstanding performance, including good cycling stability and high power density, may be able to handle the energy problems [1,2]. Supercapacitors can be divided into electrical double-layer capacitors and pseudocapacitors [3,4]. Due to the higher specific capacitance and larger energy density of pseudocapacitors compared to electrical double-layer capacitors, researchers have paid more attention to the materials of pseudocapacitors [5,6].

There are many pseudocapacitive materials, including conducting polymers [7,8], metal oxides and their composites [9,10]. Metal oxides exhibit high specific capacitance, but their electrical conductivity and rate capability are too poor to satisfy the requirements for commercialization. Therefore, transition metal sulfides with higher electrical conductivity than metal oxides are employed as pseudocapacitive materials. Facing this situation, some researchers use transition metal sulfides as pseudocapacitive materials. Cobalt sulfides have good electrical conductivity, high specific capacitance and excellent cycling stability, and will be an outstanding material for pseudocapacitors [11]. Tang *et al.* prepared CoS₂-reduced graphene oxide nanocomposite using the solvothermal method which suggests a specific capacitance of 331 F·g⁻¹ at a current density of 0.5 A·g⁻¹ [12]. Cobalt sulfide nanoparticles were also synthesized through a hydrothermal route and demonstrated a specific capacitance of 478.75 F·g⁻¹ at a scan rate of 5 mV·s⁻¹ [13]. Meanwhile, cobalt sulfide nanotubes were prepared by a hydrothermal method and exhibited a specific capacitance of 285 F·g⁻¹ at a current density of 0.5 A·g⁻¹ [14]. This research indicates that cobalt sulfides possess excellent pseudocapacitive properties. However, the above methods are complex and harmful to the environment, and still also

exhibit deficient properties such as low capacitance as well as bad cycling stability. This inspires us to search further for the synthesis and pseudocapacitive performance of cobalt sulfide. Herein, Co_9S_8 particles are compounded by a mechanical alloying method; it shows high specific capacitance and excellent cycling stability, so cobalt sulfide could serve as an outstanding material for pseudocapacitors.

2. Materials and Methods

2.1. Materials Synthesis

The synthesis of Co_9S_8 contains two processes. Firstly, Co powder (purity 99.9%, 300 mesh) and excess sulphur powder (purity 99.5%) were used as raw material to synthesize Co_9S_8 precursor by the mechanical alloying method using planetary ball mill (QM-3SP04, Nanjing NanDa Instrument Plant, Nanjing, China) and stainless steel milling balls, this process was conducted under an Ar atmosphere. The ball-to-powder weight ratio is 20:1, milling 8 h at temperature of 25 °C and the rotating speed is 450 r·min⁻¹. Secondly, the Co_9S_8 precursor was calcined at 500 °C for 4 h to get pure Co_9S_8 phase.

2.2. Structure Characterization and Electrochemical Measurement

Microstructure and morphology were investigated by X-ray diffraction (XRD, Rigaku, Beijing, China), field emission scanning electron microscopy (SEM, JSM-6701F, JEOL, Tokyo, Japan) and transmission electron microscope (TEM, JEM-2010, JEOL, Toyko, Japan). The elemental surface composition was analyzed by X-ray photoelectron spectroscopy (XPS, PHI 5700, ESCA, ULVAC NINGBO Co., Ltd, Ningbo, China). DSC-TGA (SDT Q600, Perkin Elmer, Shanghai, China) analysis was measured under a N_2 atmosphere. Electrochemical tests were measured by electrochemical working station (CHI 660D, CH instruments, Inc., Austin, TX, USA) with three electrodes system in 2 moles/liter KOH solution electrolyte, a platinum sheet as counter-electrode and a saturated calomel electrode as reference electrode.

3. Results and Discussion

The Co_9S_8 precursor is characterized by XRD to assure its components (in Figure 1a); most of the peaks are coherent with the standard pattern of Co_9S_8 (JCPDS card No. 86-2273). However, several impurity peaks of CoS (JCPDS card No. 75-0605) appeared, indicating the existence of the CoS impurity. To obtain pure Co_9S_8 , the precursor is calcined at a high temperature. The optimum calcination temperature is determined by DSC-TGA (as shown in Figure 1b). It shows one main weight loss interval and two heat exchange peaks between 0 and 400 °C. The exothermic peak observed around 110 °C is ascribed to the crystal polymorphic transformation of CoS to Co_9S_8 , and the further crystallization of the Co_9S_8 . The main weight loss at about 300 °C is mainly due to the evaporation of surplus sulfur which comes from the transformation of CoS to Co_9S_8 . This could be further identified by the obvious endothermic peak around 320 °C in the DSC curve. When the temperature exceeds 400 °C, the weight loss of the material can hardly be seen, suggesting that the crystallization process is nearly complete. Therefore, Co_9S_8 precursor is calcined at 500 °C to obtain pure Co_9S_8 . Figure 1c shows the XRD pattern of the Co_9S_8 . The peaks are coherent with the standard pattern of Co_9S_8 (JCPDS card No. 86-2273); eight strong diffraction peaks are observed at 2θ values of 15.454°, 29.838°, 31.198°, 39.554°, 47.576°, 68.08°, 73.205°, and 76.779°, and they can be ascribed to the (111), (311), (222), (331), (511), (440), (731), and (800) crystal planes. The results indicate the successful synthesis of pure Co_9S_8 phase after calcination. XPS is used to further analyze the chemical composition and valence state of Co_9S_8 . Figure 1d illustrates that the complete survey XPS spectrum of the Co_9S_8 contains O 1s, C 1s, Co 2p, and S 2p peaks. The O peaks can be ascribed to the physically and chemically adsorbed oxygen from the air. The high resolution Co 2p XPS spectrum (Figure 1e) shows Co 2p_{3/2}, Co 2p_{1/2}, and two satellites peaks. The fitting for the Co 2p_{3/2} peak reveals the presence of two peaks at 779.1 eV and 781.9 eV, and that of the Co 2p_{1/2} peak also reveals two peaks at 794.1 eV and 798.1 eV, which are ascribed to the existence of the Co^{3+} and Co^{2+} state, respectively. The S 2p spectrum (Figure 1f)

is fitted into three peaks; the peaks at 161.8 eV and 163.8 eV are correspond to S 2p_{2/3} and S 3p_{1/2}, respectively. Another is the peak at 168.5 eV which is generated by O adsorbed on the surface of S. The results suggest that Co₉S₈ is successfully prepared. SEM images of Co₉S₈ precursor and Co₉S₈ particles are shown in Figure 1g, which illustrate that the Co₉S₈ precursor and Co₉S₈ have granular shapes, and no obvious aggregation is found after calcination. Combined with the results of TEM (Figure 1i), there is a large amount of voids between the particles, which can serve as a buffer for the electrolyte so that the electrode materials can be maximally infiltrated by the electrolyte, leading to excellent pseudocapacitive properties.

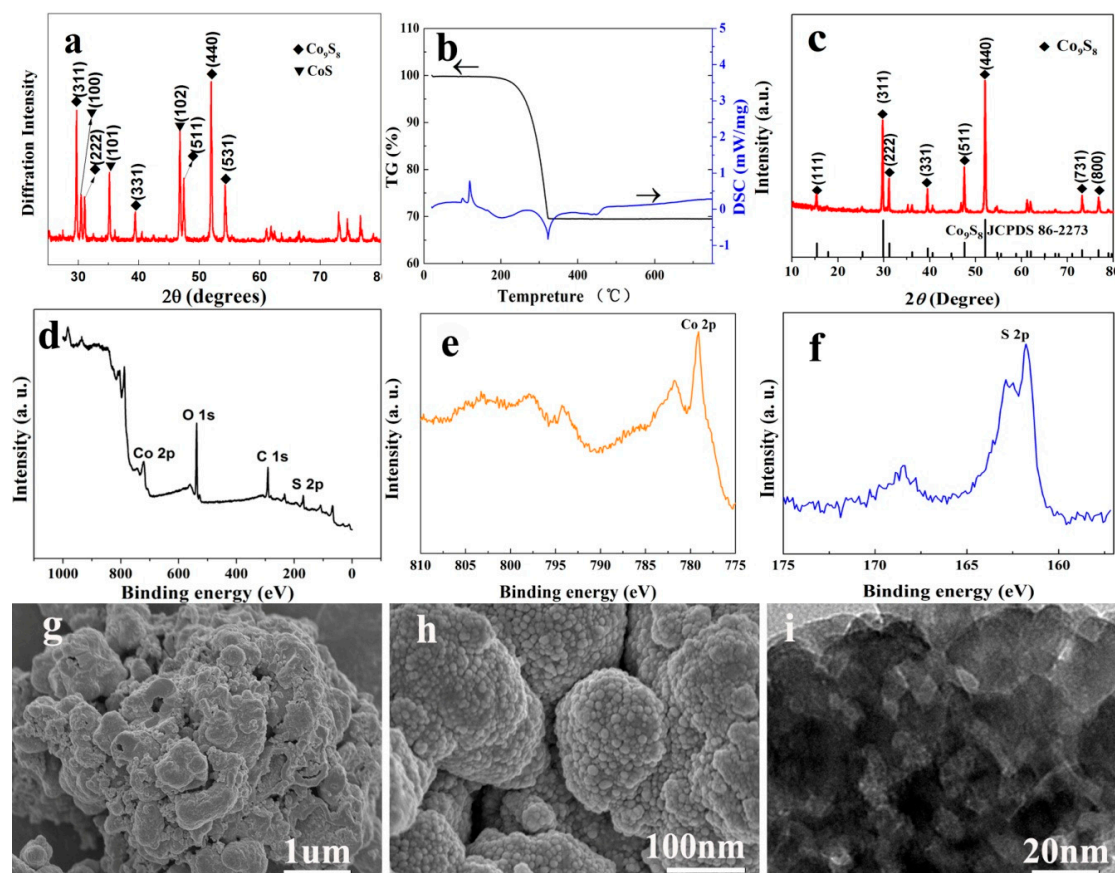


Figure 1. (a) XRD pattern and (b) DSC-TGA curve of the Co₉S₈ precursor. (c) XRD pattern of Co₉S₈. (d) Overall XPS, (e) Co 2p, and (f) S 2p XPS spectra of Co₉S₈. (g) SEM image of Co₉S₈ precursor. (h) SEM image and (i) TEM image of the Co₉S₈.

Figure 2a shows the cyclic voltammetry (CV) curves of the Co₉S₈ electrode. Obviously, they are almost symmetrically rectangular, indicating its ideal capacitive properties. With the increase of the scanning rate, the area of the CV curves became larger but its shape almost did not change, which indicates the excellent reversibility of Co₉S₈ particle electrodes. The mechanism for the charge-storage of Co₉S₈-based electrodes in alkaline solution can be explained by the following reversible process [15]:



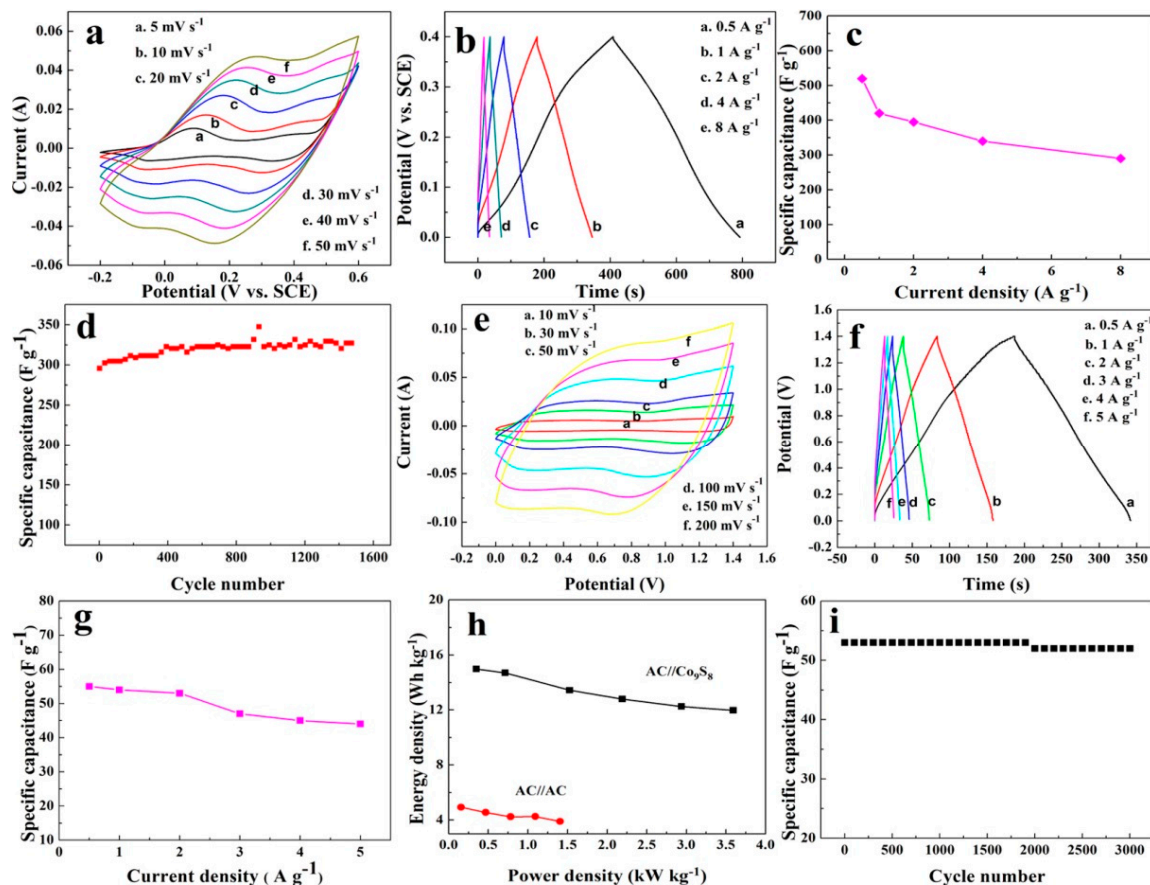


Figure 2. (a) CV curves and (b) charge/discharge curves of Co_9S_8 . (c) Specific capacitance and (d) cycling stability of Co_9S_8 . (e) CV curves and (f) charge/discharge curves of the $\text{AC}/\text{Co}_9\text{S}_8$ supercapacitor. (g) Specific capacitance, (h) Ragone plots and (i) cycle stability.

The nearly symmetrical triangular shape in the galvanostatic charge-discharge (Figure 2b) curves further indicates the ideal pseudocapacitive performance of Co_9S_8 . The specific capacitance is calculated by the equation:

$$C = \frac{I \times \Delta t}{M \times \Delta v} \quad (3)$$

where C ($\text{F}\cdot\text{g}^{-1}$) is the specific capacitance, I (A) is the discharging current and Δv (V) is the potential window. The calculated specific capacitance of the Co_9S_8 electrode (as shown in Figure 2c) is $520 \text{ F}\cdot\text{g}^{-1}$ at a current density of $0.5 \text{ A}\cdot\text{g}^{-1}$, and 56% of that is reserved when the current density is increased to $8 \text{ A}\cdot\text{g}^{-1}$. The results indicate the high specific capacitances and good rate capability of the Co_9S_8 . The cycling stability is shown in Figure 2d, where 100% of the specific capacitance remains after cycling 1500 cycles, indicating excellent cycling stability. Ascribed to the excellent pseudocapacitive properties of Co_9S_8 , an $\text{AC}/\text{Co}_9\text{S}_8$ asymmetric capacitor is assembled. In Figure 2e, the CV curves are nearly symmetrically rectangular and the shape changed very little with the increase of the scanning rate, indicating an excellent and ideal pseudocapacitive performance of the $\text{AC}/\text{Co}_9\text{S}_8$. The galvanostatic charge-discharge curves are also very close to the zig-zag (Figure 2f), showing that the Faraday reaction of $\text{AC}/\text{Co}_9\text{S}_8$ is highly reversible. The specific capacitance of the $\text{AC}/\text{Co}_9\text{S}_8$ capacitor is $55 \text{ F}\cdot\text{g}^{-1}$ at $0.5 \text{ A}\cdot\text{g}^{-1}$, and 80% of this value is retained when the current density is increased to $8 \text{ A}\cdot\text{g}^{-1}$, exhibiting an excellent rate capability. The energy density reached $15 \text{ Wh}\cdot\text{kg}^{-1}$ (Figure 2h) and is higher than that of the AC/AC supercapacitors. The cycle stability (Figure 2i) remains at 100% after 3000 cycles, suggesting the excellent cycling stability of $\text{AC}/\text{Co}_9\text{S}_8$. The above results indicate that the Co_9S_8

exhibits an ideal pseudocapacitive performance and the mechanical alloying is an excellent approach to fabricating metal sulfide materials for supercapacitors.

4. Conclusions

Co_9S_8 particles are prepared by a mechanical alloying method and used as a material for asymmetric supercapacitors. It shows excellent and ideal pseudocapacitive performance, including excellent rate capability with 80% of the specific capacitance retention when the current density increases from 0.5 to 8 $\text{A}\cdot\text{g}^{-1}$ and also outstanding cycling stability with the specific capacitance remaining at 100% after 1500 cycles. The excellent electrochemical properties mean that Co_9S_8 is a promising pseudocapacitive material and mechanical alloying is an excellent approach to fabricating metal sulfide materials with excellent pseudocapacitive properties.

Acknowledgments: This work is supported by the National Natural Science Foundation of China (No. 21403099), and the Natural Science Foundation of Gansu Province (No. 145RJZA193).

Author Contributions: Bo Li: sample preparation, and writing the manuscript. Yuxia Hu and Jiajia Li: material testing and data analysis. Maocheng Liu and Lingbin Kong: modification-Polish. Yumei Hu and Long Kang: paper examination.

Conflicts of Interest: The authors declare no conflict of interest.

References

1. Mondal, A.K.; Su, D.W.; Chen, S.Q.; Zhang, J.Q.; Ung, A.; Wang, G.X. Microwave-assisted synthesis of spherical $\beta\text{-Ni(OH)}_2$ superstructures for electrochemical capacitors with excellent cycling stability. *Chem. Phys. Lett.* **2014**, *610*, 115–120. [[CrossRef](#)]
2. He, G.Y.; Li, J.H.; Chen, H.Q.; Shi, J.; Sun, X.Q.; Chen, S.; Wang, X. Hydrothermal preparation of $\text{Co}_3\text{O}_4@\text{graphene}$ nanocomposite for supercapacitor with enhanced capacitive performance. *Mater. Lett.* **2012**, *82*, 61–63. [[CrossRef](#)]
3. Wang, Y.L.; Chang, B.B.; Guan, D.X.; Pei, K.M.; Chen, Z.; Yang, M.S.; Dong, X.P. Preparation of nanospherical porous NiO by a hard template route and its supercapacitor application. *Mater. Lett.* **2014**, *135*, 172–175. [[CrossRef](#)]
4. Wang, H.; Köster, T.K.J.; Trease, N.M.; Ségalini, J.; Taberna, P.L.; Simon, P.; Gogotsi, Y.; Grey, C.P. Real-Time NMR Studies of Electrochemical Double-Layer Capacitors. *J. Am. Chem. Soc.* **2011**, *133*, 19270–19273. [[CrossRef](#)] [[PubMed](#)]
5. Lei, Z.B.; Sun, X.X.; Wang, H.J.; Liu, Z.H.; Zhao, X.S. Platelet CMK-5 as an Excellent Mesoporous Carbon to Enhance the Pseudocapacitance of Polyaniline. *ACS Appl. Mater. Interfaces* **2013**, *5*, 7501–7508. [[CrossRef](#)] [[PubMed](#)]
6. Chen, W.; Rakhi, R.B.; Alshareef, H.N. Morphology-Dependent Enhancement of the Pseudocapacitance of Template-Guided Tunable Polyaniline Nanostructures. *J. Phys. Chem. C* **2013**, *117*, 15009–15019. [[CrossRef](#)]
7. Chen, H.C.; Chen, S.; Fan, M.Q.; Li, C.; Chen, D.; Tian, G.L.; Shu, K.Y. Bimetallic nickel cobalt selenides: A new kind of electroactive material for high-power energy storage. *J. Mater. Chem. A* **2015**, *3*, 23653–23659. [[CrossRef](#)]
8. Li, S.G.; Teng, F.; Chen, M.D.; Li, N.; Hua, X.; Wang, K.; Li, M. Interesting electrochemical properties of novel three-dimensional Ag_3PO_4 tetrapods as a new super capacitor electrode material. *Chem. Phys. Lett.* **2014**, *601*, 59–62. [[CrossRef](#)]
9. Kurra, N.; Wang, R.Q.; Alshareef, H.N. All conducting polymer electrodes for asymmetric solid-state supercapacitors. *J. Mater. Chem. A* **2015**, *3*, 7368–7374. [[CrossRef](#)]
10. Rauda, I.E.; Augustyn, V.; Dunn, B.; Tolber, S.H. Enhancing Pseudocapacitive Charge Storage in Polymer Templated Mesoporous Materials. *Accounts Chem. Res.* **2013**, *46*, 1113–1124. [[CrossRef](#)] [[PubMed](#)]
11. Rakhi, R.B.; Alhebshi, N.A.; Anjum, D.H.; Alshareef, H.N. Nanostructured cobalt sulfide-on-fiber with tunable morphology as electrodes for asymmetric hybrid supercapacitors. *J. Mater. Chem. A* **2014**, *2*, 16190–16198. [[CrossRef](#)]

12. Tang, J.H.; Shen, J.F.; Li, N.; Ye, M.X. A free template strategy for the synthesis of CoS₂-reduced graphene oxide nanocomposite with enhanced electrode performance for supercapacitors. *Ceram. Int.* **2014**, *40*, 15411–15419. [[CrossRef](#)]
13. Krishnamoorthy, K.; Veerasubramani, G.K.; Kim, S.J. Hydrothermal synthesis, characterization and electrochemical properties of cobalt sulfide nanoparticles. *Mat. Sci. Semicond. Proc.* **2015**, *40*, 781–786. [[CrossRef](#)]
14. Wan, H.Z.; Ji, X.; Jiang, J.J.; Yu, J.W.; Miao, L.; Zhang, L.; Bie, S.W.; Chen, H.C.; Ruan, Y.J. Hydrothermal synthesis of cobalt sulfide nanotubes: The size control and its application in supercapacitors. *J. Power Sources* **2013**, *243*, 396–402. [[CrossRef](#)]
15. Yin, L.; Wang, L.Q.; Liu, X.H.; Gai, Y.S.; Su, L.H.; Qu, B.H.; Gong, L.Y. Ultra-Fast Microwave Synthesis of 3D Flower-Like Co₉S₈ Hierarchical Architectures for High-Performance Supercapacitor Applications. *Eur. J. Inorg. Chem.* **2015**, *14*, 2457–2462. [[CrossRef](#)]



© 2016 by the authors; licensee MDPI, Basel, Switzerland. This article is an open access article distributed under the terms and conditions of the Creative Commons Attribution (CC-BY) license (<http://creativecommons.org/licenses/by/4.0/>).